ARTICLE

ACS chemical biology

Exploiting Structural Analysis, *in Silico* Screening, and Serendipity To Identify Novel Inhibitors of Drug-Resistant Falciparum Malaria

Tina Dasgupta[†,∥], Penchit Chitnumsub[‡], Sumalee Kamchonwongpaisan[‡], Cherdsak Maneeruttanarungroj[‡], Sara E. Nichols[§], Theresa M. Lyons[¶], Julian Tirado-Rives[¶], William L. Jorgensen[¶], Yongyuth Yuthavong[‡], and Karen S. Anderson[†,*]

[†]Department of Pharmacology, Yale University School of Medicine, 333 Cedar Street, New Haven, Connecticut 06520, [‡]BIOTEC Central Research Unit, National Science and Technology Development Agency, Science Park, 113 Phaholyothin Road, Klong Luang, Pathumthani 12120, Thailand, [§]Interdepartmental Program in Computational Biology and Bioinformatics, Yale University, 300 George Street Suite 501, New Haven, Connecticut 06511, and [¶]Department of Chemistry, Yale University, 225 Prospect Street, New Haven, Connecticut 06520. [∥]Present address: Department of Medicine, Memorial Sloan-Kettering Cancer Center, 1275 York Ave., New York, NY 10065.

ABSTRACT *Plasmodium falciparum* thymidylate synthase-dihydrofolate reductase (TS-DHFR) is an essential enzyme in folate biosynthesis and a major malarial drug target. This bifunctional enzyme thus presents different design approaches for developing novel inhibitors against drug-resistant mutants. We performed a high-throughput *in silico* screen of a database of diverse, drug-like molecules against a non-active-site pocket of TS-DHFR. The top compounds from this virtual screen were evaluated by *in vitro* enzymatic and cellular culture studies. Three compounds active to 20 μM IC_{50}'s in both wildtype and antifolate-resistant *P. falciparum* parasites were identified; moreover, no inhibition of human DHFR enzyme was observed, indicating that the inhibitory effects appeared to be parasite-specific. Notably, all three compounds had a biguanide scaffold. However, relative free energy of binding calculations suggested that the compounds might preferentially interact with the active site over the screened non-active-site region. To resolve the two possible modes of binding, co-crystallization studies of the compounds complexed with TS-DHFR enzyme were performed. Surprisingly, the structural analysis revealed that these novel, biguanide compounds do indeed bind at the active site of DHFR and additionally revealed the molecular basis by which they overcome drug resistance. To our knowledge, these are the first co-crystal structures of novel, biguanide, non-WR99210 compounds that are active against folate-resistant malaria parasites in cell culture.

*Corresponding author, karen.anderson@yale.edu.

Received for review June 7, 2008 and accepted December 3, 2008.

Published online January 16, 2009

10.1021/cb8002804 CCC: $40.75

Malaria is an infectious disease caused by *Plasmodium* spp. parasites and remains an epidemic of sweeping socioeconomic consequence in tropical countries (*1, 2*). Between 1 and 3 million lives are lost annually, and over 40% of the world's population is at risk of contracting malaria, with some 350 million new infections each year (*2*). Notably, *P. falciparum* infections account for over 90% of malaria-related mortality (*2*). The past decade has seen a 25% increase in mortality from malaria in Africa alone, due in large part to a rise in drug-resistant parasites (*2*).

The history of malaria treatment is one of acquired drug resistance and toxic side effects. There is known, widespread resistance to chloroquine, mefloquine, atovaquone, proguanil, and pyrimethamine (*3–5*). Artemisinin compounds, developed from ancient Chinese herbals, are the only antimalarials to which known resistance has not yet been identified (*3*). With the introduction of each new antimalarial drug, resistance has emerged more quickly than with the last (*2, 6, 7*). Novel, less toxic, and more specific non-artemisinin treatments are urgently needed to curb this global epidemic (*2*).

Antifolates such as pyrimethamine and cycloguanil are active-site inhibitors of the malarial dihydrofolate reductase (DHFR) enzyme and have been used successfully to treat falciparum malaria (*3*). They prevent the conversion of dihydrofolate (H_2-folate) to tetrahydrofolate (H_4-folate) by DHFR (*3*). Interestingly, unlike in humans where TS and DHFR are encoded as two discrete enzymes, the malarial DHFR is encoded on the same

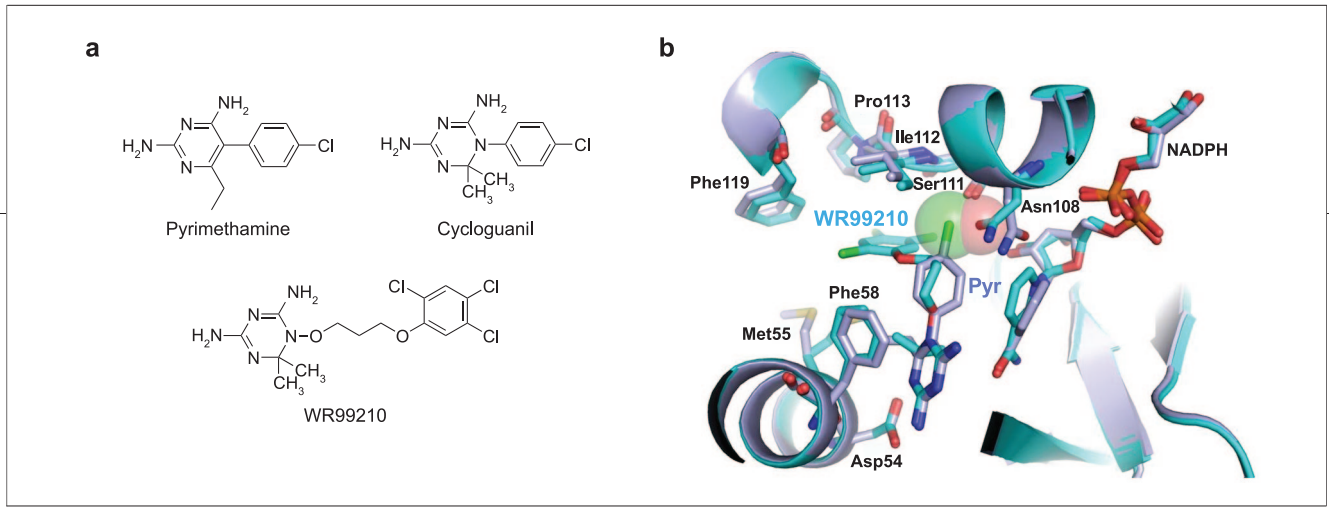

Figure 1. Known antifolate antimalarials and their mode of binding to *P. falciparum* DHFR. a) Structure of WR99210 compared to those of the clinically used antifolates pyrimethamine and cycloguanil. b) WR99210 (WR, cyan) binds successfully to the active site of the clinically important, drug-resistant N51I/C59R/S108N/I164L "quadruple" mutant of *P. falciparum* DHFR. Unlike pyrimethamine (Pyr, purple), WR99210 avoids steric hindrance with Asn108, which clashes with the *p*-chlorophenyl ring of pyrimethamine, the DHFR inhibitor in FansidarTM. NADPH, an essential cofactor in the conversion of H2-folate to H4-folate by DHFR, is shown bound to the DHFR active site as well.

polypeptide chain as the thymidylate synthase (TS) enzyme, which catalyzes the upstream reaction of converting methylene tetrahydrofolate (CH_2H_4-folate) to H_2-folate. This bifunctional thymidylate synthase-dihydrofolate reductase (TS-DHFR) enzyme is the target of antifolate drug design in *P. falciparum*. (TS-DHFR is a functional designation as dihydrofolate is produced at TS and utilized at DHFR; this enzyme is also commonly referred to as DHFR-TS in the literature because the DHFR domain is N-terminal to TS.)

Although resistance to antifolates in *P. falciparum* emerged soon after their introduction, pyrimethamine continues to be used today, in combination therapy with sulfadoxine (sulfadoxine-pyrimethamine or SP, trade name Fansidar) for malaria prophylaxis in pregnant women (*9*). In addition, SP combined with amiodaquine or artesenuate remains the first-line therapy for uncomplicated *P. falciparum* malaria in many parts of sub-Saharan Africa (*5*). It should be noted that competitive inhibitors of *P. falciparum* DHFR such as pyrimethamine are routinely used in combination therapy (*5*).

Antifolate resistance in *P. falciparum* TS-DHFR is caused by point mutations in the DHFR active site (*10*). The first mutation thought to occur is S108N, followed by C59R, then N51I, and finally I164L; each subsequent mutation progressively decreases the binding of both H_2-folate (the natural substrate) and pyrimethamine as a result of structural changes in the DHFR active site (*8*). The K_i values for pyrimethamine for the double mutant C59R/S108N and N51I/C59R/S108N/I164L DHFR are 50-fold and >500-fold less inhibitory, respectively, than for wildtype (WT) (1.5 nM) (*11*). Note that these K_i's are only for the monofunctional *P. falciparum* DHFR enzyme and reaction. Pyrimethamine-resistant DHFR mutations are found throughout West and Central Africa and Asia (*5*).

Several attempts have been made to develop novel antifolates that bind to the active site of the clinically important quadruple mutant of *P. falciparum* TS-DHFR. One of these, the dihydrotriazene WR99210 (Figure 1, panel a), has a subnanomolar K_i value for the WT, double mutant, and quadruple mutant DHFRs (*8*). Structural studies have demonstrated that WR99210 is highly effective against the quadruple mutant because it lacks the *p*-chlorophenyl moiety of antifolates like pyrimethamine and has a flexible linker, both of which enable it to avoid steric clash with Asn108 (*8*). WR99210 is also bound within the "substrate space", the essential space within the active site that cannot undergo major conformational rearrangements if H_2-folate binding (and thus catalytic activity) are to be preserved (*8*) (Figure 1, panel b). Unfortunately, the poor oral bioavailability of WR99210 prevents its clinical use (*12*). To develop novel *P. falciparum* DHFR active-site inhibitors, molecular docking studies using derivatives of WR99210 (*13*) or pyrimethamine (*14*) are underway in some laboratories (*15*). There have also been reports of molecular docking studies using homology models of *P. falciparum* DHFR (*16*).

The bifunctional malarial TS-DHFR enzyme has non-active regions that both flank and tether these two active sites together, and which have no homology to the human TS and DHFR enzymes (*17*). As *in vitro* kinetic studies have shown, the non-active-site regions of parasitic TS-DHFR enzymes can play a significant role in modulating catalysis (*17*). In the malaria enzyme specifically, *E. coli* complementation studies with the *P. falciparum* TS and DHFR enzymes have also suggested an important role for these distant structural regions (*18, 19*).

The structural and kinetic properties of *P. falciparum* TS-DHFR therefore suggest different approaches toward

novel inhibitor design. One method would involve developing new active-site inhibitors that are equally effective against WT and drug-resistant parasites. A second method would target the non-active-site regions, which have no known homology to the human host. To our knowledge, however, no current efforts are focused on the development of novel, non-WR99210 scaffolds or on the extensive non-active-site regions of *P. falciparum*TS-DHFR to develop novel, parasite-specific antifolates.

The 89 amino acid long linker (from residues 232 to 320) in *P. falciparum* TS-DHFR encodes significant secondary structure and at least an RNA-binding site (*20*). Complementation studies suggest a role for this junctional region in modulating activity and association between the TS and DHFR domains (*18, 19*). Therefore, the linker could serve as an interesting target for molecular docking and virtual screening studies for a potential novel, non-active-site inhibitor of *P. falciparum*TS-DHFR.

In this study, we performed virtual screening studies of the Maybridge Hitfinder library of diverse, drug-like compounds (*21*) that could bind with moderate (midmicromolar) affinity to a non-active-site pocket within the linker region of *P. falciparum* TS-DHFR. Whereas previous molecular docking studies have been reported on a homology model of the *P. falciparum* DHFR (*16, 22, 23*) before the three-dimensional structure was available, our study involves a virtual screen of the completed crystal structure of the *P. falciparum* bifunctional TS-DHFR enzyme. Using *in vitro* enzyme screening, as well as malarial cell culture studies, we identified three lead compounds with similar activity against WT and antifolate-resistant *P. falciparum* parasites in culture. Significantly, these three compounds had non-WR99210 scaffolds, and further computational analysis was used to evaluate their interaction with the non-active-site pocket as well as the DHFR active site. Virtual free energy of binding calculations predicted that these lead compounds would actually preferentially interact with the DHFR active site, instead of the linker region screened by molecular docking. Structural studies were carried out to obtain the structure of the inhibitors bound to the bifunctional *P. falciparum* TS-DHFR enzyme and distinguish between the two plausible sites for inhibitor binding. Serendipity played a role since co-crystallography studies confirmed that these lead inhibitors bound to the DHFR active site for WT and drug-resistant TS-DHFR enzyme rather than the non-active pocket initially targeted by virtual screening. These structural studies also revealed the molecular mechanism for the compounds' interaction with the quadruple, drug-resistant form of the TS-DHFR enzyme and offer a new avenue to exploit for future development of targeted, structure-guided antimalarial therapy.

RESULTS AND DISCUSSION

We describe the identification of a novel biguanide scaffold that is active in cell culture against the clinically important antifolate-resistant mutant of *P. falciparum* TS-DHFR. Using enzymatic and cell culture assays to screen the "hits" from our molecular docking studies, we identified three compounds, RJF 001302, RJF 00670, and RJF 00719, with around 20 μM inhibition in *P. falciparum* pyrimethamine-resistant DHFR enzyme in *in vitro* kinetic studies. Our data also showed these compounds to be active in both WT and quadruple mutant *P. falciparum* cell culture. As kinetic studies regarding the pattern of inhibition were inconclusive and the compounds had a biguanide moiety somewhat akin to WR99210 (a known competitive inhibitor of *P. falciparum* DHFR), we pursued free energy of binding calculations using MM-GB/SA (molecular mechanics and the generalized Born model and solvent accessibility) (*24*). These results suggested that all three compounds preferred to bind to the DHFR active site, compared to the non-active-site pocket that was originally targeted. Since we could not decisively assign the RJF compounds as non-active-site inhibitors, we proceeded with structural studies of these inhibitors complexed with *P. falciparum* TS-DHFR enzyme for definitive determination of the mode of binding. Interestingly, despite our virtual screening data, co-crystallization studies of inhibitor complexed with the WT and pyrimethamine-resistant quadruple mutant enzymes confirmed that these compounds do indeed bind to DHFR active site. Importantly, however, the RJF compounds avoid steric clash with Asn108, a key residue that hinders existing antifolates such as pyrimethamine from binding the drug-resistant mutant enzymes. Also, several key interactions between inhibitor and the DHFR active site, shown previously to be essential in successful antifolates such as WR99210 or pyrimethamine (*8*), are retained by the RJF compounds, even in the quadruple mutant enzyme. Each of these points is elaborated upon below.

Virtual Screening of a Non-Active-Site Pocket in *P. falciparum* TS-DHFR. We screened 16,000 compounds from the Maybridge HitFinder library against the crystal structure of WT *P. falciparum* TS-DHFR using Glide SP (Supplementary Figure 1). The top 14 compounds identified by this screen are shown in Supplementary Table 1 with their corresponding Glide scores and chemical structures, and a summary flowchart of the screening process is provided in Supplementary Figure 2. Overlaying the top "hit" compounds in the crossover region showed that the ligands had different binding modes, implying that they occupy one of several "spaces" within the non-active-site pocket (Figure 2). These inhibitors were characterized with QikProp and showed favorable predicted ADME properties (*25*) (Supplementary Table 2).

The Maybridge HitFinder compound database was screened because it comprises the chemical diversity of the entire Maybridge compound library, prescreens the compounds for Lipinski rules (*26*), and is commercially available to over 90% purity (*21*). The Glide SP score is a soft scoring function used to identify ligands likely to bind to a target protein, thereby minimizing false negatives. The most heavily weighted items in determining the Glide score are van der Waals interactions and lipophilic contact, and compounds with lower scores are predicted to bind more tightly to the target protein. Scores ranged from -9.32 to -8.50, which is within the normal range of expected scores for moderate affinity (midmicromolar) compounds from Glide SP (*27*).

Because this was an initial attempt at small molecule binding in the non-active-site pocket, we set a large boundary condition (Supplementary Figure 1) and favored results with diversity in shape and binding mode of the inhibitor (Figure 2). QikProp was used to check important physical properties of the top hits from this screening, as it predicts log *P*, log *S*, and Caco-2 (physical properties useful in inhibitor optimization in the drug design process). Compounds with molecular weight < 450, log $P < 5$, log $S > -5$, and pCaco > 25 are considered to have favorable lead-compound-like properties (*25*).

Virtual screening methods have limitations due to approximations used in the scoring function, as well as measures taken to simplify the conformational search space to reduce computation time for the thousands of screened compounds (*28*). Another limitation of this virtual screening study was the molecular docking of a predicted doubly charged biguanide moiety in the screened compounds, although experimental evidence suggests that these biguanides are monoprotonated at physiological pH (*29, 30*). Furthermore, kinetic evidence suggests that the current crystal structure of WT *P. falciparum* TS-DHFR may not be in its most active conformation as the TS active site is not doubly liganded (*17*). As this was the initial virtual screening of the non-active-site pocket, these molecular docking studies were done with minimal experimental evidence about which residues in the non-active site are functionally important or how protein conformation would adjust to inhibitor binding at the non-active site.

***In Vitro* Enzymatic Assays of Inhibitor Assay.** Using a spectrophotometric assay, which follows the consumption of NADPH at 340 nm, we screened the hits for inhibition of the bifunctional TS-DHFR and DHFR activities. Several compounds exhibited intrinsic absorbance or display signal attenuation at 340 nm, and the activity of these compounds was further examined under steady-state conditions using a radiolabeled assay for bifunctional TS-DHFR and DHFR activity. A number of hits also precipitated in buffer conditions, even in high/low salt conditions and in very acidic or very basic pHs, and those compounds insoluble in reaction buffer were excluded from the analysis.

The compounds were initially screened for inhibition of the bifunctional TS-DHFR reaction using both a spectrophotometric and a radiolabeled assay. As the radiolabeled assay showed a buildup of H_2-folate in the reaction products at early time points for RJF 01302, we also screened these compounds for DHFR activity in the bifunctional enzyme. Of the top 14 compounds tested, we found three active compounds to inhibit the DHFR reaction in the bifunctional enzyme: RJF 00670, RJF 01302, and RJF 00719. They did not inhibit the human DHFR enzyme at 500 μmol L^{-1} concentrations. Kinetic studies to determine a pattern of inhibition (competitive or noncompetitive) in the bifunctional enzyme using both a radiolabeled and spectrophotometric assay were somewhat inconclusive.

This combination of these analyses identified three compounds of interest, all of which inhibited DHFR (but not TS) activity in the WT bifunctional TS-DHFR enzyme. Because of difficulties with expressing sufficient quantities of the full-length, bifunctional quadruple mutant (N51I/C59R/S108N/I164L) *P. falciparum* TS-DHFR en-

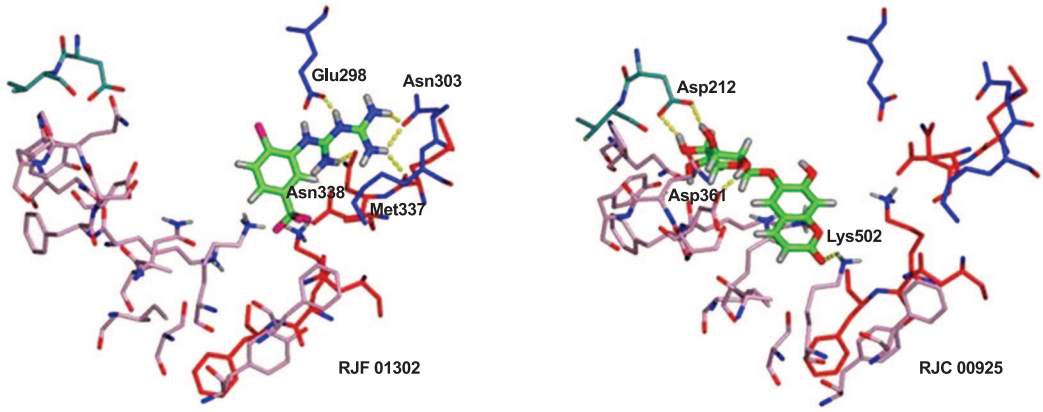

Figure 2. Glide parameters were optimized to maximize surface binding flexibility in the non-active-site pocket, as well as binding to both TS (red/pink) and DHFR (blue) domains. Here, RJF 01302 and RJC 00925 are shown binding to different regions of the non-active-site pocket.

zyme, we used monofunctional constructs of *P. falciparum* WT and quadruple mutant DHFR for further *in vitro* enzyme assays to determine an accurate, comparative IC_{50} for the DHFR reaction in WT and quadruple mutant enzymes. These results are summarized in Table 1, and the corresponding curves are shown in Supplementary Figure 3.

Interestingly, all three of these compounds, RJF 01302, RJF 00670, and RJF 00719, contain a biguanide scaffold. (The RJF compounds were developed in the chemistry laboratory of Ray J. Froude at Maybridge (now Thermofisher Scientific, Tintagel) in the early 1980s. They were originally produced as intermediates en route to synthesizing aminotriazenes and later were developed into a "series" of drug-like molecules (*1*).) The IC_{50} of these compounds was ~500 μM for the bifunctional reaction, predominately reflecting the TS reaction, but ~20 μM for the DHFR reaction, as determined by spectrophotometric assays. It is of note that other compounds containing a biguanide scaffold (see Supplementary Table 1) were not inhibitory: in some of these cases, solubility was limiting (RJF 00587, RJF 00729), but in other cases the lack of inhibitory effect is puzzling (RJF 00600). RJF 01059 had weak activity against the DHFR (but not bifunctional TS-DHFR reaction) and was therefore not pursued for further analysis. We also tested biguanides (RDR 01651, RJF 00541, and RDR 003335) that were not identified by the Glide screen but were Maybridge HitFinder compounds related to RJF 01302. None of these latter compounds were active in *in vitro* enzymatic assays (data not shown). Excitingly, when RJF 00719, RJF 00670, and RJF 01302 were assayed for their activity in the monofunctional construct of *P. falciparum* DHFR, they showed similar inhibition in both WT enzyme and the strongly pyrimethamine-resistant quadruple mutants of the enzyme.

Although an obvious limitation of the IC_{50} determination was that we assayed for activity using a monofunctional DHFR enzyme, the comparative results are valid as both the WT and quadruple mutant enzyme were monofunctional in this assay and determining inhibitor activity using a monofunctional DHFR enzyme is a well-accepted, standard assay in the *P. falciparum* antifolate literature (*31*). While standard steady-state competition assays performed using the spectrophotometric assay suggested these compounds had a noncompetitive pattern of inhibition, these data were obviously limited by the inherent absorbance of the compounds at 340 nm, as well as the signal attenuation described above. Therefore, free energy of binding calculations were pursued to predict whether the RJF compounds preferred the DHFR active site to the non-active-site pocket in the linker region (see below).

Cell Culture Assays of Inhibitor Activity. To determine activity in both WT and antifolate-resistant cell culture, the three RJF compounds were assayed for activity in *P. falciparum* parasites with either WT DHFR enzyme

TABLE 1. IC_{50} values of RJF compounds in *in vitro* enzyme and cell culture assays of WT and quadruple mutant *P. falciparum* TS-DHFR

	IC_{50} (μM)			
	In WT DHFR *in vitro* assay	In quadrupole mutant DHFR *in vitro* assay	In WT parasite cell culture	In quadrupole mutant cell culture
RJF 00719	21 ± 2	40 ± 2	20 ± 2	19.9 ± 0.5
RJF 01302	29.9 ± 0.5	39.1 ± 0.5	22 ± 3	20 ± 2
RJF 00670	17 ± 2	20 ± 2	>50	>50

(TM4/8.2) or the quadruple mutant DHFR enzyme (V1/S or N51I/C59R/S108N/I164L). The *P. falciparum* parasite cell culture (TM4/8.2 and V1/S, respectively) in the erythrocytic stage of the life cycle was performed using a standard [^{3}H]-hypoxanthine incorporation assay (*32*).

The compounds demonstrated similar activity in both WT and quadruple mutant parasites in the erythrocytic stages (Table 1). The higher IC_{50} of RJF 00670 in cell culture could possibly be explained by degradation or metabolic instability. More importantly, the fact that the IC_{50} values were relatively similar for the DHFR monofunctional enzyme and cell culture assays for two of the three compounds suggested that DHFR might indeed be the major target of the RJF compounds.

Inhibition of parasite replication during erythrocytic stages is an important indicator of activity, because the majority of *P. falciparum* parasites in an infected human host reside within the erythrocyte. It is intraerythrocytic replication and subsequent extravasation of erythrocytes that causes the fevers, chills, anemia, and secondary organ damage characteristic of falciparum malaria (*33*). However, inhibition of the liver stages (sporozoite phase) by the RJF compounds, as well as their oral bioavailability and toxicology, must be further examined in animal models of malaria (like *P. berghei*). Evaluation of inhibition of the sporozoite phase of this parasite is important for determining the use of these lead compounds for malaria prophylaxis (*34*).

Evaluation of the Relative Free Energy of Binding To Determine the Preferred Binding Site for RJF Compounds. To investigate whether these lead compounds were binding at the non-active-site pocket or the DHFR active site, relative free energies of binding were calculated on the basis of their Glide poses. WR99210, the ligand from the crystal structure used in the docking studies (PDB id 1j3i), was used as a control. The relative free energies of binding ($\Delta\Delta G_{\text{active site}-\text{non-active site}}$) for WR99210, RJF 01302, RJF 00670, and RJF 00719 were −33, −31, −56, and −22 kcal mol^{-1}, respectively. These computational data indicated that WR99210 and the RJF compounds all preferred binding the DHFR active site over the non-active-site pocket in the linker region (Figure 3).

Conventional docking studies could not be used to compare these binding energies, given the 45 Å distance between the sites. MM-GB/SA methods to estimate approximate relative free energies of binding are considered an efficient way to post process compounds after high-throughput virtual screening, avoiding more time-consuming free energy simulations (*24*). Traditionally, energies are used relatively in one site, comparing multiple ligands. Here, multiple sites for individual ligands were examined to determine specificity rather than to find a top lead. Known DHFR active-site inhibitor WR99210 was used as a control, as the calculations should indicate that it prefers binding the DHFR active site. In this case, trends are more important than magnitudes because of necessary approximations made due to the distance between the two sites (around 45 Å) and the size of the bifunctional homodimer. While MM-GBSA methods tend to quantitatively overestimate binding free energies (*35*), the calculations provide a qualitative indication that the RJF compounds (as well as the known DHFR active-site inhibitor control, WR99210) prefer binding the active site of *P. falciparum* DHFR. The RJF compounds likely ranked high in the original screen of the non-active-site pocket in the linker region because of their charged (protonated) states and the multiple charged residues at both the DHFR active site and the non-active-site pocket (Figure 2).

Co-crystallization of Inhibitors with *P. falciparum* WT and Quadruple Mutant TS-DHFR. Given that computational methods suggested that the DHFR active site was the target site, structural studies were pursued. We were able to co-crystallize the inhibitor RJF 00670 with the full-length, bifunctional quadruple mutant of *P. falciparum* TS-DHFR to 2.56 Å resolution (PDB id 3DG8; Figure 4, panel a) and RJF 01302 with the WT enzyme to 2.70 Å resolution (PDB id 3DGA; Figure 4, panel b). We were also able to crystallize the co-complex of TS-DHFR with RJF 00719 but unfortunately could not see enough of the electron density to report the complete cocomplex structure. This is likely due in part to solubility limitations with RJF00719, indicating perhaps that the binding site was not completely saturated.

Both RJF01302 and RJF00670 co-crystallized at the active site of the DHFR enzyme, indicating that virtual free energy of binding studies, which predicted binding of RJF compounds at the DHFR active site, corresponded well with the crystallography data (Figure 3). The com-

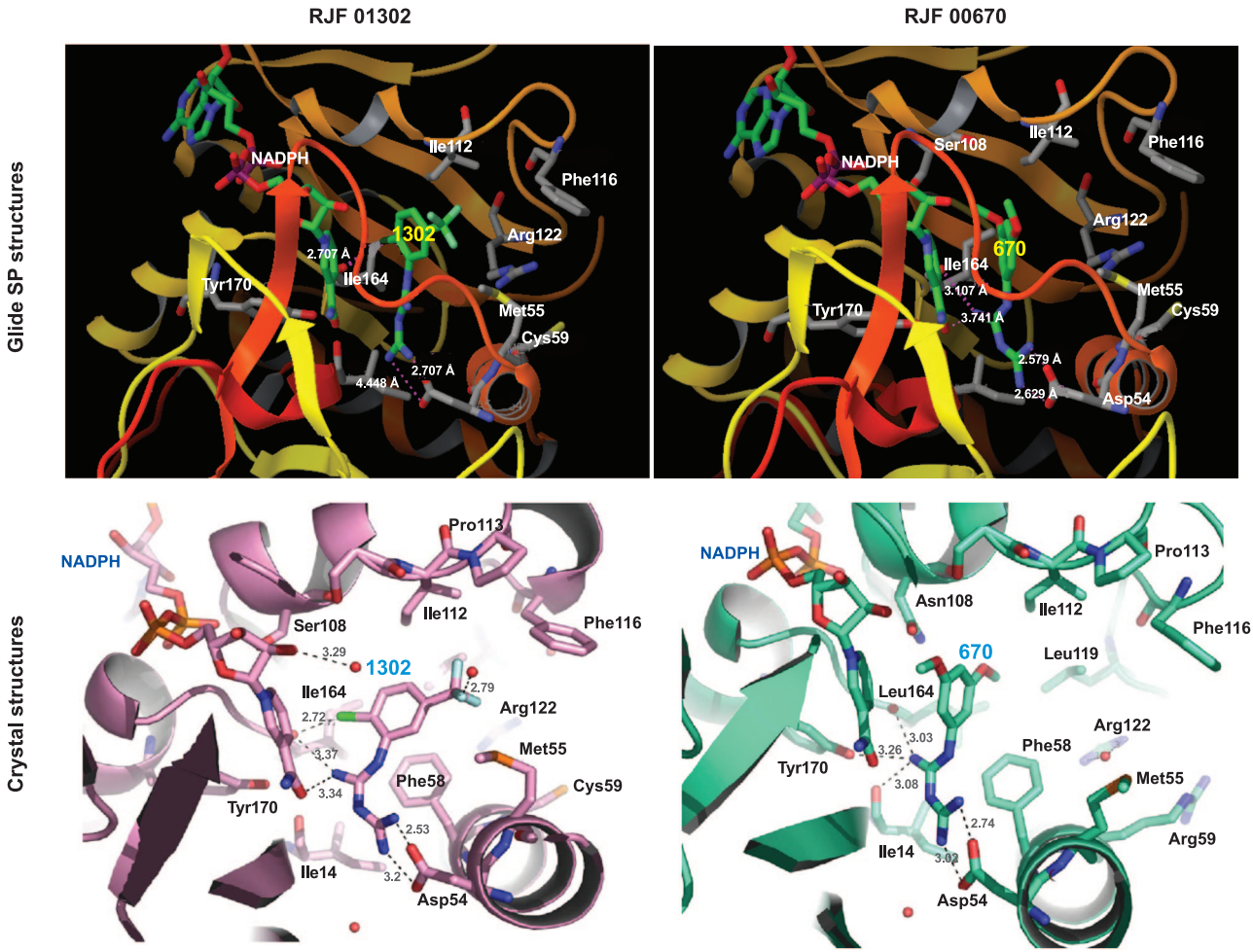

Figure 3. MM/GBSA calculations of free energy of binding predict that RJF compounds bind to the active site of *P. falciparum* DHFR (upper panel), as confirmed by co-crystallization studies (lower panel).

plete electron density of both ligands was observed, despite the relatively high B factors. The protein−ligand interactions formed between the active site residues of DHFR and the inhibitors were calculated using LigPlot and are shown in Supplementary Table 3. We also performed an analysis of the common interactions formed between WR99210 and the quadruple mutant DHFR, as well as between pyrimethamine and the WT DHFR, and compared these interactions to those formed by the RJF compounds. These interactions are summarized in Supplementary Table 3 and their implications are discussed below. Data collection and refinement statistics are shown in Table 2, and F_o-F_c maps are shown in Supplementary Figures 4 and 5.

Although these results were unanticipated by our initial virtual screening studies, a low-micromolar novel scaffold that binds to the DHFR active site of and has activity in both WT and quadruple mutant *P. falciparum* parasites remains an important finding. When the co-crystal structures of RJF 00670 and RJF 01302 are superimposed (Figure 4, panel c) and the hydrophobic, van der Waals, and H-bond interactions formed between inhibitor and DHFR active site are examined closely, several interesting observations are made.

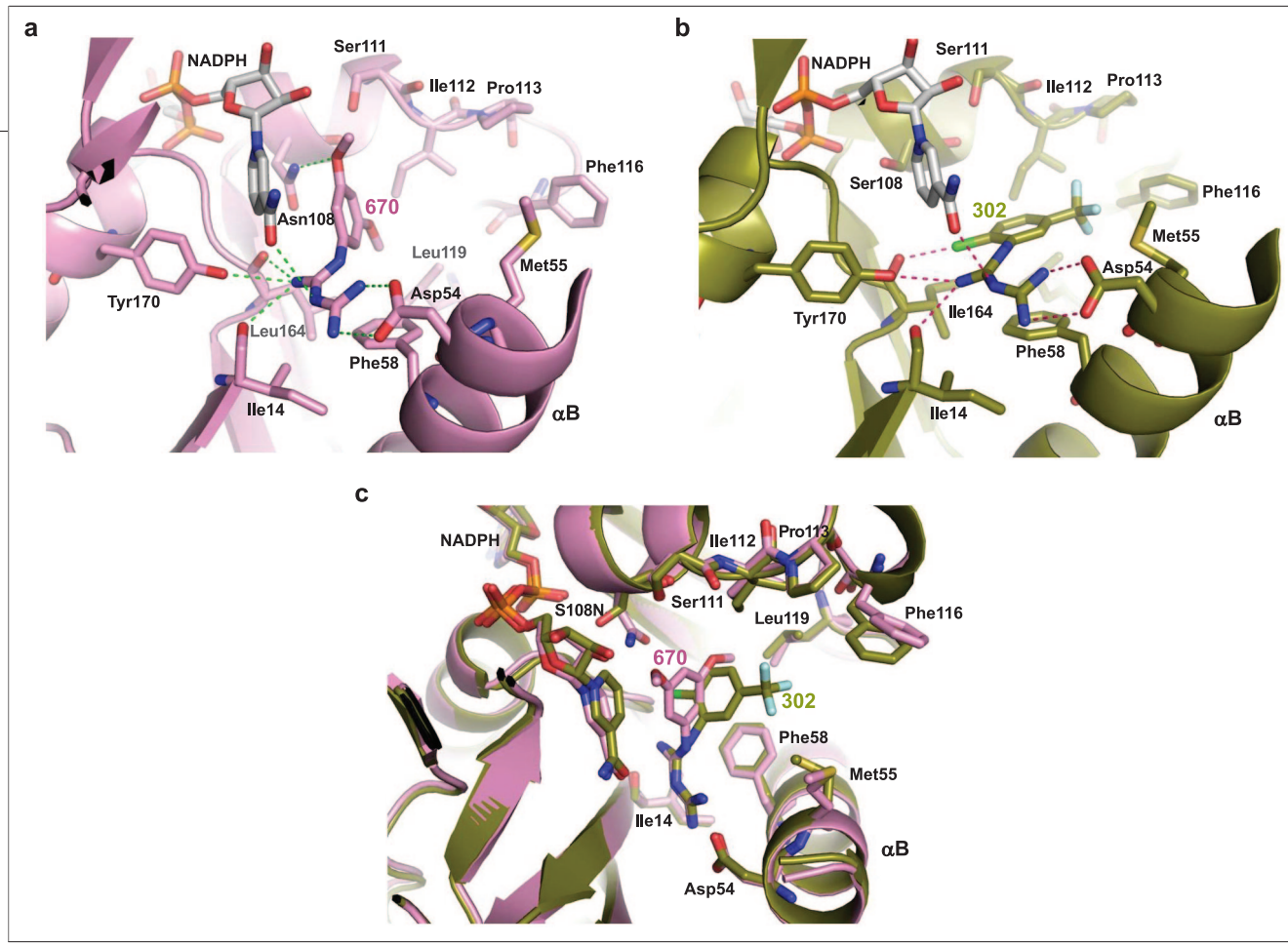

Figure 4. Structural studies demonstrate the binding site of RJF compounds. a) Co-crystallization studies show RJF 00670 to be bound at the DHFR active site of the quadruple mutant of *P. falciparum* TS-DHFR enzyme. The DHFR active site of this co-crystal was in its fully liganded conformation as NADPH was also bound. Hydrogen bonds between the inhibitor and the enzyme active site are shown with green dashed lines. b) Co-crystallization studies show RJF 01302 to be bound at the DHFR active site of the WT *P. falciparum* TS-DHFR enzyme. The DHFR active site of this co-crystal was in its fully liganded conformation as NADPH was also bound. Hydrogen bonds between the inhibitor and the enzyme active site are shown with red dashed lines. c) Superimposition of the X-ray crystal structures of RJF 00670 (shown in purple) and of RJF 01302 (shown in green) bound to the DHFR active site of *P. falciparum* TS-DHFR.

First and most importantly, both RJF 00670 and RJF 01302 are not sterically hindered by Asn108, the point mutation essential for pyrimethamine resistance. (RJF 01302 was co-crystallized with the WT enzyme, and this was determined by aligning this structure to the active site of the quadruple mutant.) That the RJF compounds also avoid this steric clash, just as WR99210 but unlike pyrimethamine, suggests a common mechanism for overcoming antifolate resistance in malarial DHFR and is encouraging with respect to their potential as promising antifolate scaffolds for further lead optimization (Figure 5).

Second, in the antifolate inhibitor literature on *P. falciparum* TS-DHFR, there has been much analysis to discern the interactions that are essential between enzyme and inhibitor. In addition to Ser108, another such important residue (which lies at the opposite ends of the hydrophobic substrate space) that interacts with WR99210 and pyrimethamine is Asp54 (on α helix B) (*8*). Chemically, the RJF compounds vary from WR99210 by lacking a cyclic guanidinium ring and the dimethyl group. Despite that, both RJF 00670 and RJF 01302 form hydrogen bonds with the carboxyl side chain of Asp54 and the backbone carbonyl of Ile164 (another common mutation in the quadruple mutant of pyrimethamine-resistant DHFR). Furthermore, as shown in Supplementary Table 3, the RJF compounds also make polar interactions with Ile14, Tyr170, and Cys15 and van der Waals contact with residues Phe58, Ile112, Leu119, Met55, Cys15, and Ala16 at the DHFR active site. Despite being $\sim$100 g mol^{-1} smaller in molecular weight than WR99210, the RJF compounds thus form many of the same interactions considered to make WR99210 and the pterin ring of the natural substrate H_2F bind so tightly

TABLE 2. Data collection and refinement statistics for co-crystal structures of RJF 00670 bound to the quadruple mutant *P. falciparum* TS-DHFR and RJF 01302 bound to the WT *P. falciparum* TS-DHFR

	RJF 00670 co-crystallized with quadruple mutant TS-DHFR[a]	RJF 01302 co-crystallized with WT TS-DHFR[a]
Space group	$P2_12_12_1$	$P2_12_12_1$
Unit cell parameter (Å)	56.516 155.404 165.183 90 90 90	57.377 156.015 164.567 90 90 90
Resolution (Å)	50−2.56 (2.65−2.56)	30−2.70 (2.80−2.70)
No. observed/unique reflections	189,861 (45,686)	205,888 (41,531)
Completeness	98.0% (95.0%)	99.8% (99.9%)
$I/\sigma I$	19.86 (6.36)	17.18 (4.41)
R_{merge}	6.6% (26.5%)	8.0% (29.9%)
No. of molecules or asymmetric units	2	2
Refinement resolution (Å)	30−2.56	30−2.70
R_{fac}/R_{free}	0.198/0.239	0.205/0.256
Reflections used in refinement	45,613 (95.4%)	41,385 (99.7%)
Working set	43,291 (90.5%)	39,304 (94.7%)
Test set	2,322 (4.9%)	2,081 (5.0%)
Number of glycines	48	48
Most favored regions[b]	843	836
Additional allowed regions[b]	147	150
Generously allowed regions[b]	10	14
Disallowed regions[b]	0	0
Average B factors of enzyme (Å^2)	45.96	44.32
Average B factors of RJF, chains A and B (Å^2)	50.1 and 89.2	79.0 and 89.2
Average B factors of NADPH, chains A and B (Å^2)	48.8 and 89.6	34.3 and 75.9

[a]Numbers in parentheses are for the highest resolution bin. [b]Number of residues by Ramachandran plot.

and specifically within the substrate space of the quadruple mutant DHFR.

A third critical observation is that the aromatic ring of the RJF compounds forms very few interactions with the residues of the active site (Figure 4, panels a and b). This finding reaffirms the usefulness of the RJF series as potential lead compounds since functional groups can be added easily to this ring, especially in a position *meta* or *para* to the bis-imine.

Do These Inhibitors Specifically Target *P. falciparum* DHFR? Several lines of evidence suggest that *P. falciparum* DHFR is at least one of the primary targets of the RJF compounds. First, the IC_{50} in cell culture and in enzyme assays are approximately equivalent, suggesting that DHFR may be the primary target of these inhibitors. Also, these compounds co-crystallize at the active site of both WT and quadruple mutant *P. falciparum* DHFR. Though the RJF series are small lead compounds, it should be noted that the human DHFR enzyme is not inhibited by these compounds at 500 μmol L^{-1} concentrations. "Folate effect" studies are often used to demonstrate folate pathway inhibition by sulfa drugs. However, the utility of similar folate antagonism studies remains unclear for target validation of DHFR inhibitors in *P. falciparum*, given the complexities of folate salvage and catabolism pathways in the *Plasmodium* parasite and the tremendous folate reserve of *Plasmodium* parasites even after several reinvasions (*36*). For example, folate can be cleaved to pterin-6-aldehyde and *p*-amino-benzoylglutamate, byproducts utilized in folate biosynthesis, while exogenous intact folates are also alternatively salvaged and utilized by the parasite (*37, 38*). *P. falciparum* may additionally have putative folate transporters, whose candidate genes, MAL8P1.13 and PF11_0172, we have previously identified (*39*). For example, folic acid and folinic acid could not be used to reverse the effect of even pyrimethamine in *P. knowlesi* (*40*) or of WR99210 in *P. falciparum*, though the refrac-

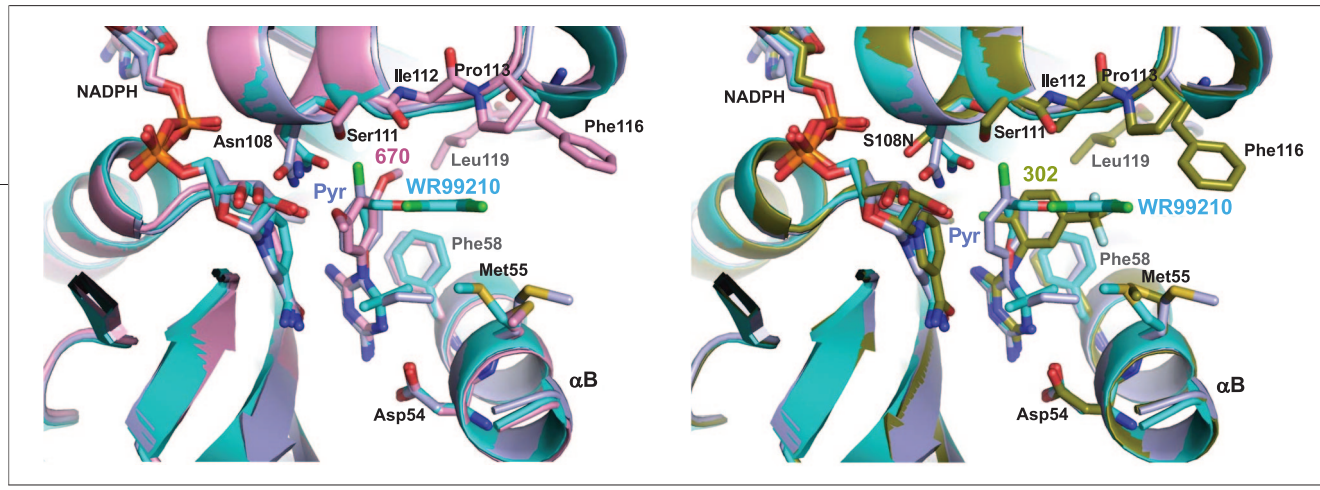

Figure 5. Overlays of the active sites of *P. falciparum* DHFR demonstrating that RJF compounds overcome drug resistance by avoiding steric clash with Asn 108. RJF 01302 (green, right panel), RJF 00670 (purple, left panel), pyrimethamine (navy blue), and WR99210 (cyan) are shown bound to the DHFR active site. The structures overlaid are from pdb codes 1J3K (quadruple mutant with WR99210) and 1J3J (double mutant with pyrimethamine) and the co-crystal structures described in this paper.

tory effect depended on the strain and experimental approach used (*41–43*). Consequently, experiments using the "folate effect" to validate targets of inhibition such as DHFR are often difficult to interpret for the purpose of drawing definitive conclusions.

Summary and Implications for Potential Novel Antifolates Based on the RJF Scaffold. Biguanides are routinely used clinically and are recognized as safe, well-tolerated, and highly effective antidiabetic therapy agents (*44*). Additionally, guanidines have been implicated before in the development of *E. coli* DHFR inhibitors (*45, 46*), and at least one cyclic biguanide has been shown to have anti-plasmodial activity at 10 μmol L^{-1} when tested in the WT 3d7 strain (*47*). However, this is the first report of guanidine scaffolds co-crystallized with a drug-resistant mutant of the malarial TS-DHFR enzyme. Our data both demonstrate that RJF compounds have similar activity in cell culture in WT and antifolate-resistant parasites, as well as potentially suggest a common mechanism for how antifolates overcome drug resistance in malarial DHFR. Furthermore, these co-crystal structures can enable structure-guided development of novel inhibitors that maximize key active site interactions by the addition of functional groups to the RJF scaffold. Future directions will focus on testing these inhibitors in human cell culture, as well as developing subtractive *in silico* filters to select non-active-site inhibitors that do not bind the DHFR active site.

In the face of growing mortality, new antimalarials are urgently needed. RJF compounds therefore hold the exciting potential of serving as novel scaffolds for development of targeted, structure-guided antimalarial therapy.

METHODS

Additional details for each section are available in Supporting Information.

Molecular Docking Studies. With close examination of the linker region in the structure of *P. falciparum* TS-DHFR (PDB id 1j3i), we identified a pocket within the linker region defined by contributing residues from the linker, DHFR, and TS domains, with the rationale that binding of a small molecule to this linker might disrupt DHFR and/or TS function (Figure 2). The Maybridge Hitfinder Library (Maybridge, U.K.), containing a subset of 16,000 molecules representing the chemical diversity of the entire Maybridge database (*21*), was virtually screened against this pocket using Glide Standard Precision v 3.5 (Schrödinger, New York), a third generation molecular docking program (*27*). Additional details have been previously reported (*48*).

***In Vitro* Enzymatic Assays of Inhibitor Activity.** The hits from the Glide molecular docking studies were screened using a spectrophotometric assay for the *P. falciparum* TS-DHFR enzyme, as well as an assay using tritiated substrate and rapid chemical quench methodology for TS-DHFR activity, both performed under steady-state conditions and previously described (*17*). The IC_{50} was determined by plotting rate versus inhibitor concentration and determining inhibitor concentration at half-maximal velocity (v_{max}). Detailed methods have been previously published (*17*).

Approximate Relative Free Energy of Binding To Determine the Preferred Binding Site. Because of the similarity of the active compounds identified by *in vitro* screening to known active-site inhibitors, computational techniques were used to determine relative binding affinities. On the basis of experimental results (*29, 30*), we determined that all three compounds should be in a monoprotonated ionization state, in contrast to the bisprotonated ionization state generated by LigPrep. The correct forms of the three RJF compounds and known competitive inhibitor WR99210 were redocked in both the active site and in the non-active-site pocket of the linker region. Relative free energies of binding were then calculated on the basis of complexes from this second docking. Additional details are outlined in Supporting Informaion.

Cell Culture Assays of Inhibitor Activity. The RJF compounds were tested in erythrocytic stages of *P. falciparum* parasite with WT and with N51I/C59R/S108N/I164L quadruple mutant of DHFR. Detailed methods were as previously described (*49, 50*).

Co-crystallization Studies and Data Analysis. The RJF compounds were co-crystallized in the absence of the H_2-folate, the natural substrate of DHFR. RJF 01302 was co-crystallized with the WT *P. falciparum* TS-DHFR enzyme, and RJF 00670 was co-crystallized with the quadruple mutant. We also attempted to co-crystallize the RJF compounds in the presence of cycloguanil, an active-site inhibitor of DHFR. Blocking the active site of DHFR

was attempted to see if the RJF compound would bind at an alternative binding site such as the non-active-site pocket in the linker region. Otherwise, methods for co-crystallization of compounds with *P. falciparum* TS-DHFR, X-ray diffraction data collection, and analysis to determine the actual binding site of the compound were as previously published (*51*). Atomic coordinates have been deposited in the Protein Data Bank.

Acknowledgment: This work was supported in part by National Institutes of Health Grant AI 44630 (to KSA), an NIH Medical Student Training Program grant to the Yale M.D.-Ph.D. Program (to T.D.), a Doctoral Research Award from the Canadian Institutes of Health Research (to T.D.), an international research scholarship from the Howard Hughes Medical Institute (to S.K.), NIH Grants AI 44616 and GM32136 (to W.L.J.), and a grant from Medicines for Malaria Ventures MMV99/0099 (to Y.Y.). We gratefully acknowledge the use of the National Synchrotron Radiation Research Center Beamline BL13B1 (Taiwan) and the work of Roonglawan Ratanachak (National Science and Technology Development Agency, Thailand) in drug-resistant parasite cell culture studies. Also, we would like to thank Jeff Saunders (Schrödinger, Portland, OR), Raymond Chung (Patent and Trade Office, Washington, DC), and Walter (Eddie) Martucci for helpful discussions in the preparation of this manuscript.

Supporting Information Available: This material is free of charge *via* the Internet.

REFERENCES

1. Greenwood, B. M., Fidock, D. A., Kyle, D. E., Kappe, S. H., Alonso, P. L., Collins, F. H., and Duffy, P. E. (2008) Malaria: progress, perils, and prospects for eradication, *J. Clin. Invest. 118*, 1266–1276.
2. Greenwood, B. M., Bojang, K., Whitty, C. J., and Targett, G. A. (2005) Malaria, *Lancet 365*, 1487–1498.
3. Rieckmann, K. H. (2006) The chequered history of malaria control: are new and better tools the ultimate answer? *Ann. Trop. Med. Parasitol. 100*, 647–662.
4. Greenwood, D. (1995) Conflicts of interest: the genesis of synthetic antimalarial agents in peace and war, *J. Antimicrob. Chemother. 36*, 857–872.
5. World Health Organization. (2006) *Guidelines for the Treatment of Malaria*, WHO Press, Geneva. Accessed online Feb, 2008.
6. Centers for Disease Control and Prevention. (2004) *The History of Malaria, an Ancient Disease*. Accessed online Mar, 2008. http://www.cdc.gov/malaria/history/index.htm#ancienthistory.
7. Centers for Disease Control and Prevention. (2004) *The Impact of Malaria, a Leading Cause of Death Worldwide*. Accessed online Mar, 2008. http://www.cdc.gov/malaria/impact.htm.
8. Yuvaniyama, J., Chitnumsub, P., Kamchonwongpaisan, S., Vanichtanankul, J., Sirawaraporn, W., Taylor, P., Walkinshaw, M. D., and Yuthavong, Y. (2003) Insights into antifolate resistance from malarial DHFR-TS structures, *Nat. Struct. Biol. 10*, 357–365.
9. World Health Organization. (2004) *A Strategic Framework for Malaria Prevention and Control during Pregnancy in the Africa Region*, WHO Regional Office for Africa, Brazzaville. Accessed online Feb, 2008.
10. Peterson, D. S., Walliker, D., and Wellems, T. E. (1988) Evidence that a point mutation in dihydrofolate reductase-thymidylate synthase confers resistance to pyrimethamine in falciparum malaria, *Proc. Natl. Acad. Sci. U.S.A. 85*, 9114–9118.
11. Sardarian, A., Douglas, K. T., Read, M., Sims, P. F., Hyde, J. E., Chitnumsub, P., Sirawaraporn, R., and Sirawaraporn, W. (2003) Pyrimethamine analogs as strong inhibitors of double and quadruple mutants of dihydrofolate reductase in human malaria parasites, *Org. Biomol. Chem. 1*, 960–964.
12. Warhurst, D. C. (2002) Resistance to antifolates in *Plasmodium falciparum*, the causative agent of tropical malaria, *Sci. Prog. 85*, 89–111.
13. Hunt, S. Y., Detering, C., Varani, G., Jacobus, D. P., Schiehser, G. A., Shieh, H. M., Nevchas, I., Terpinski, J., and Sibley, C. H. (2005) Identification of the optimal third generation antifolate against *P. falciparum* and *P. vivax*, *Mol. Biochem. Parasitol. 144*, 198–205.
14. Fogel, G. B., Cheung, M., Pittman, E., and Hecht, D. (2008) Modeling the inhibition of quadruple mutant *Plasmodium falciparum* dihydrofolate reductase by pyrimethamine derivatives, *J. Comput.-Aided Mol. Des. 22*, 29–38.
15. Yuthavong, Y. (2002) Basis for antifolate action and resistance in malaria, *Microbes Infect. 4*, 175–182.
16. Rastelli, G., Pacchioni, S., Sirawaraporn, W., Sirawaraporn, R., Parenti, M. D., and Ferrari, A. M. (2003) Docking and database screening reveal new classes of *Plasmodium falciparum* dihydrofolate reductase inhibitors, *J. Med. Chem. 46*, 2834–2845.
17. Dasgupta, T., and Anderson, K. S. (2008) Probing the role of parasite-specific, distant structural regions on communication and catalysis in the bifunctional thymidylate synthase-dihydrofolate reductase from *Plasmodium falciparum*, *Biochemistry 47*, 1336–1345.
18. Shallom, S., Zhang, K., Jiang, L., and Rathod, P. K. (1999) Essential protein-protein interactions between *Plasmodium falciparum* thymidylate synthase and dihydrofolate reductase domains, *J. Biol. Chem. 274*, 37781–37786.
19. Wattanarangsan, J., Chusacultanachai, S., Yuvaniyama, J., Kamchonwongpaisan, S., and Yuthavong, Y. (2003) Effect of N-terminal truncation of *Plasmodium falciparum* dihydrofolate reductase on dihydrofolate reductase and thymidylate synthase activity, *Mol. Biochem. Parasitol. 126*, 97–102.
20. Zhang, K., and Rathod, P. K. (2002) Divergent regulation of dihydrofolate reductase between malaria parasite and human host, *Science 296*, 545–547.
21. Thermofisher Scientific Inc. *Maybridge Hitfinder Library*. Accessed Jun 2, 2008.
22. Toyoda, T., Brobey, R. K., Sano, G., Horii, T., Tomioka, N., and Itai, A. (1997) Lead discovery of inhibitors of the dihydrofolate reductase domain of *Plasmodium falciparum* dihydrofolate reductase-thymidylate synthase, *Biochem. Biophys. Res. Commun. 235*, 515–9.
23. McKie, J. H., Douglas, K. T., Chan, C., Roser, S. A., Yates, R., Read, M., Hyde, J. E., Dascombe, M. J., Yuthavong, Y., and Sirawaraporn, W. (1998) Rational drug design approach for overcoming drug resistance: application to pyrimethamine resistance in malaria, *J. Med. Chem. 41*, 1367–70.
24. Guimaraes, C. R., and Cardozo, M. (2008) MM-GB/SA rescoring of docking poses in structure-based lead optimization, *J. Chem. Inf. Model. 48*, 958–970.
25. Jorgensen, W. L., and Duffy, E. M. (2002) Prediction of drug solubility from structure, *Adv. Drug Deliv. Rev. 54*, 355–636.
26. Lipinski, C. A., Lombardo, F., Dominy, B. W., and Feeney, P. J. (2001) Experimental and computational approaches to estimate solubility and permeability in drug discovery and development settings, *Adv. Drug Deliv. Rev. 46*, 3–26.
27. (2005) *Glide*, version 3.5, Schrodinger, LLC, New York.
28. Shoichet, B. K. (2004) Virtual screening of chemical libraries, *Nature 432*, 862–865.
29. Amigó, J., Martínez-Calatayud, J. M., Cantarero, A, and Debaerdemaeker, T. (1988) Molecular structure of 1-(2-sulfoethyl)biguanide, *Acta Crystallogr., Sect C: Cryst. Struct. Commun. 44*, 1452–1454.
30. Hariharan, M., Rajan, S. S., and Srinivasan, R. (1989) Structure of metformin hydrochloride, *Acta Crystallogr.* 911–913.
31. Yuthavong, Y., Yuvaniyama, J., Chitnumsub, P., Vanichtanankul, J., Chusacultanachai, S., Tarnchompoo, B., Vilaivan, T., and Kamchonwongpaisan, S. (2005) Malarial (*Plasmodium falciparum*) dihydrofolate reductase-thymidylate synthase: structural basis for antifolate resistance and development of effective inhibitors, *Parasitology 130*, 249–259.

32. Desjardins, R. E., Canfield, C. J., Haynes, J. D., and Chulay, J. D. (1979) Quantitative assessment of antimalarial activity *in vitro* by a semiautomated microdilution technique, *Antimicrob. Agents Chemother. 16*, 710–718.
33. Schuster, F. L. (2002) Cultivation of plasmodium spp. *Clin. Microbiol. Rev. 15*, 355–364.
34. de Andrade-Neto, V. F., da Silva, T., Lopes, L. M., do Rosario, V. E., de Pilla Varotti, F., and Krettli, A. U. (2007) Antiplasmodial activity of aryltetralone lignans from *Holostylis reniformis*, *Antimicrob. Agents Chemother. 51*, 2346–2350.
35. Kormos, B. L., Benitex, Y., Baranger, A. M., and Beveridge, D. L. (2007) Affinity and specificity of protein U1A-RNA complex formation based on an additive component free energy model, *J. Mol. Biol. 371*, 1405–1419.
36. Wang, P., Wang, Q., Aspinall, T. V., Sims, P. F., and Hyde, J. E. (2004) Transfection studies to explore essential folate metabolism and antifolate drug synergy in the human malaria parasite *Plasmodium falciparum*, *Mol. Microbiol. 51*, 1425–1438.
37. Krungkrai, J., Webster, H. K., and Yuthavong, Y. (1989) *De novo* and salvage biosynthesis of pteroylpentaglutamates in the human malaria parasite, *Plasmodium falciparum*, *Mol. Biochem. Parasitol. 32*, 25–37.
38. Wang, P., Brobey, R. K., Horii, T., Sims, P. F., and Hyde, J. E. (1999) Utilization of exogenous folate in the human malaria parasite *Plasmodium falciparum* and its critical role in antifolate drug synergy, *Mol. Microbiol. 32*, 1254–1262.
39. Massimine, K. M., Doan, L. T., Atreya, C. A., Stedman, T. T., Anderson, K. S., Joiner, K. A., and Coppens, I. (2005) *Toxoplasma gondii* is capable of exogenous folate transport. A likely expansion of the BT1 family of transmembrane proteins, *Mol. Biochem. Parasitol. 144*, 44–54.
40. McCormick, G. J., Canfield, C. J., and Willet, G. P. (1971) *Plasmodium knowlesi*: *in vitro* evaluation of antimalarial activity of folic acid inhibitors, *Exp. Parasitol. 30*, 88–93.
41. Kinyanjui, S. M., Mberu, E. K., Winstanley, P. A., Jacobus, D. P., and Watkins, W. M. (1999) The antimalarial triazine WR99210 and the prodrug PS-15: folate reversal of *in vitro* activity against *Plasmodium falciparum* and a non-antifolate mode of action of the prodrug, *Am. J. Trop. Med. Hyg. 60*, 943–947.
42. Yeo, A. E., Seymour, K. K., Rieckmann, K. H., and Christopherson, R. I. (1997) Effects of folic and folinic acids in the activities of cycloguanil and WR99210 against *Plasmodium falciparum* in erythrocytic culture, *Ann. Trop. Med. Parasitol. 91*, 17–23.
43. Fidock, D. A., and Wellems, T. E. (1997) Transformation with human dihydrofolate reductase renders malaria parasites insensitive to WR99210 but does not affect the intrinsic activity of proguanil, *Proc. Natl. Acad. Sci. U.S.A. 94*, 10931–10936.
44. Stumvoll, M., Haring, H. U., and Matthaei, S. (2007) Metformin, *Endocr. Res. 32*, 39–57.
45. Mayer, S., Daigle, D. M., Brown, E. D., Khatri, J., and Organ, M. G. (2004) An expedient and facile one-step synthesis of a biguanide library by microwave irradiation coupled with simple product filtration. Inhibitors of dihydrofolate reductase, *J. Comb. Chem. 6*, 776–782.
46. Summerfield, R. L., Daigle, D. M., Mayer, S., Mallik, D., Hughes, D. W., Jackson, S. G., Sulek, M., Organ, M. G., Brown, E. D., and Junop, M. S. (2006) A 2.13 A structure of E. coli dihydrofolate reductase bound to a novel competitive inhibitor reveals a new binding surface involving the M20 loop region, *J. Med. Chem. 49*, 6977–6986.
47. Chong, C. R., Chen, X., Shi, L., Liu, J. O., and Sullivan, D. J., Jr. (2006) A clinical drug library screen identifies astemizole as an antimalarial agent, *Nat. Chem. Biol. 2*, 415–416.
48. Lyons, T. M. (2006) Structure-based Drug Design of Non-active Site Inhibitors for HIV-1 Targeting Reverse Transcriptase and Malaria Targeting *Plasmodium falciparum* Thymidylate Synthase-Dihydrofolate Reductase. Ph.D. thesis, Yale University, New Haven.
49. Kamchonwongpaisan, S., Quarrell, R., Charoensetakul, N., Ponsinet, R., Vilaivan, T., Vanichtanankul, J., Tarnchompoo, B., Sirawaraporn, W., Lowe, G., and Yuthavong, Y. (2004) Inhibitors of multiple mutants of *Plasmodium falciparum* dihydrofolate reductase and their antimalarial activities, *J. Med. Chem. 47*, 673–680.
50. Ponmee, N., Chuchue, T., Wilairat, P., Yuthavong, Y., and Kamchonwongpaisan, S. (2007) Artemisinin effectiveness in erythrocytes is reduced by heme and heme-containing proteins, *Biochem. Pharmacol. 74*, 153–160.
51. Chitnumsub, P., Yuvaniyama, J., Vanichtanankul, J., Kamchonwongpaisan, S., Walkinshaw, M. D., and Yuthavong, Y. (2004) Characterization, crystallization and preliminary X-ray analysis of bifunctional dihydrofolate reductase-thymidylate synthase from *Plasmodium falciparum*, *Acta Crystallogr., Sect. D: Biol. Crystallogr. 60*, 780–783.